We are IntechOpen,
the world's leading publisher of
Open Access books
Built by scientists, for scientists

6,900
Open access books available

185,000
International authors and editors

200M
Downloads

154
Countries delivered to

Our authors are among the

TOP 1%
most cited scientists

12.2%
Contributors from top 500 universities

CLARIVATE ANALYTICS

BOOK
CITATION
INDEX

INDEXED

WEB OF SCIENCE™

Selection of our books indexed in the Book Citation Index
in Web of Science™ Core Collection (BKCI)

Interested in publishing with us?
Contact book.department@intechopen.com

Numbers displayed above are based on latest data collected.
For more information visit www.intechopen.com

Energy Recovery in Capacitive Deionization Technology

Alberto M. Pernía, Miguel J. Prieto,
Juan A. Martín-Ramos, Pedro J. Villegas and
Francisco J. Álvarez-González

Additional information is available at the end of the chapter

Abstract

Capacitive deionization technique (CDI) represents an interesting alternative to compete with reverse osmosis by reducing energy consumption. It is based on creating an electric field between two electrodes to retain the salt ions on the electrode surface by electrostatic attraction; thus the CDI cell operates as a supercapacitor storing energy during the desalination process. Most of the CDI research is oriented to improving the electrode materials in order to increase the effective surface and ionic retention. However, if the CDI overall efficiency is to be improved, it is necessary to optimize the CDI cell geometry and the charge/discharge current used during the deionization process. A DC/DC converter is required to transfer the stored energy from one cell to another with the maximum possible efficiency during energy recovery, thus allowing the desalination process to continue. A detailed description of energy losses and the DC/DC converter used to recover part of the energy involved in the CDI process will provide the hints to optimize the efficiency of the CDI technique for water desalination. The proposed chapter presents an electric model to characterize the power losses in CDI cells and the power converter required for the energy recovery process.

Keywords: capacitive deionization, energy recovery, up-down DC/DC converter, desalination, carbon electrodes, supercapacitors

1. Introduction

Nowadays it is evident that fresh water, suitable for different types of consumption, is a resource of paramount importance and growing scarcity, although throughout modern history the fact that it is a limited resource has been overlooked. Several factors, such as

overpopulation, global warming, the increase of polluting emissions and the growing energy demand of the world productive model are at the base of numerous studies that indicate an alarming water scarcity in the medium term. Thus, some sources [1] estimate a 40% increase in water demand with respect to its availability within a period of 20 years, which makes it possible to calculate that one-third of the world's population will have access to only 50% of the amount of water necessary to cover their basic needs.

With this forecast and the potential increase of the world population, it is estimated that by 2050 a global water crisis without precedents could be established that would create very high levels of scarcity in large regions of the planet. This necessarily implies investments in the improvement of water saving and the optimization of current methods of water regeneration/purification.

Over the past decades, processes such as reverse osmosis (RO), electrodialysis and various forms of distillation, such as multi-effect distillation and multi-stage flash distillation, have reached a high level of technological and industrial maturity [2, 3], and are currently the reference processes and mostly used for the regeneration/production of drinking water on a large scale. These methods have the main drawback of high energy consumption (e.g. 4–7kWh/m^3 for RO) so that new strategies for purification are being investigated in order to reduce their consumption.

CDI technology is presented as an efficient alternative to the previously mentioned technologies, as it allows an important recovery of the energy involved in the process.

2. Capacitive deionization (CDI)

CDI technology uses an electric field created by a pair of electrodes to induce the mobility and separation of the dissolved salts in the water towards the corresponding electrodes (**Figure 1**). The salts (their ionic components) are retained at the interface between the electrode and the aqueous medium, in an electrochemical structure called double-layer. Therefore, CDI is a low-pressure desalination process where an energy recovery process can be used to minimize the energy consumption.

2.1. Operating principle

As it was mentioned, CDI technology uses the electric field created between the electrodes to retain the ions on the electrode surface by means of electrostatic attraction [4]. This accumulation of ions on the electrodes is a thermodynamically reversible process and can be eliminated in a later step, during which the electrodes are depolarized. The behavior of the structure is similar to a supercapacitor that can be charged or discharged. In order to increase the effective surface of the electrode, nanoporous carbon materials are used to cover the surface of the electrode [5–7].

The first phase of operation is called deionization or desalination phase, and more technically, the ionic adsorption phase. This phase lasts as long as it takes the equivalent capacitor to
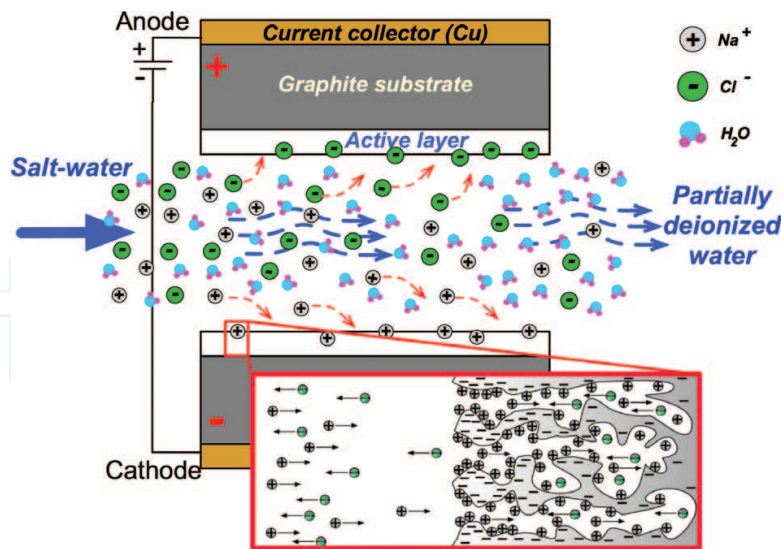
Figure 1. Schematic of ion adsorption during the polarization of electrode plates.

charge to the desired potential, always lower than 1.2 V to avoid water dissociation. The water between the electrodes will be partially deionized during this stage. During the second phase, the electrodes are depolarized or discharged while circulating a flow of water that is used to facilitate the removal of the ions adsorbed by the electrode plates, which will be evacuated in the form of a concentrate or brine. This second phase is called the regeneration or cleaning phase since it makes the electrodes be ready for a new cycle again.

This principle and mode of operation, based on alternating charge-discharge of the equivalent capacitor, suggests the use of the energy accumulated in the electrodes during the regeneration phase (once the electrodes are saturated of salt ions) to supply another deionization module that starts the desalination phase. This principle of energy reuse (transferring energy between deionization modules) implies the possibility of significantly reducing the energy consumption of the system.

The primary energy source will only have to provide the necessary amount of energy to compensate the losses that occur during the energy transfer between the CDI cells.

2.2. Membrane capacitive deionization (MCDI)

In this variant of capacitive deionization, ion-selective membranes are interposed between the electrodes and the solution. In this way, it is possible to use the polarity reversal in the electrodes periodically, drastically improving the efficiency in the cleaning phase [8, 9].

In addition, the use of membranes improves the performance of the process, since it increases the electronic efficiency, which is the ratio between the amount of salt eliminated and the amount of electric current supplied to the CDI cell to achieve that goal.

Figure 2 shows a diagram of the MCDI operation composed of two capacitive units or cells. Each of the cathodes has a cation-selective membrane interposed, and each anode has an anion-selective membrane so that the ions charged with a sign opposite to that of the electrode
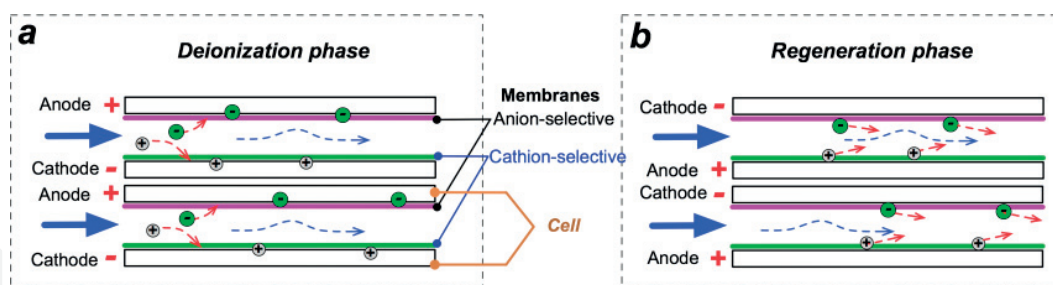
Figure 2. Schematic of a membrane capacitive deionization cell.

(or counter-ions) can move freely through the membrane, while the movement of ions with a charge of the same sign is blocked.

During the purification phase, the electrodes invert the polarity to facilitate the desorption of the adsorbed ions in the previous desalination phase. The re-adsorption of ions is avoided thanks to the barrier posed by the membranes.

In both cases, CDI or MCDI, another important parameter, is the effective electrode surface. This parameter is related to the equivalent capacitance that represents the deionization cell and, therefore, to the quantity of salt that can be adsorbed.

3. CDI module characterization

The interface between an electrically charged electrode and an electrolytic solution is a problem widely studied as part of the so-called surface phenomena. In this interface, a region of ionic accumulation is formed, commonly called electric double-layer, in which the ionic species present in the electrolytic medium are spatially distributed in a characteristic manner responding to the electronic charge present in the electrode. In this type of interfaces, it is known that the accumulated charge density depends on the voltage level of the electrode, the concentration of the solution and its chemical composition.

The double-layer name comes from the first theoretical model formulated to explain the accumulation of charge in these interfaces. In 1883, Helmholtz assumes that the electric charges in the electrode form a layer that induces another layer in the solution, of ionic character and polarity opposite to that of the electrode. In the Helmholtz model, the layer present in the solution is formed by ions intimately in contact with the outer surface of the electrode (the surface in contact with the solution) and it is assumed that there are no further interactions within the solution due to the influence of the electrode beyond this layer adjacent to the surface.

Assuming a flat electrode, the Helmholtz model is equivalent to the classical model of a flat-parallel capacitor (**Figure 3**) where A is the effective electrode surface, X_H is the distance between ions and ε_r is the permittivity.
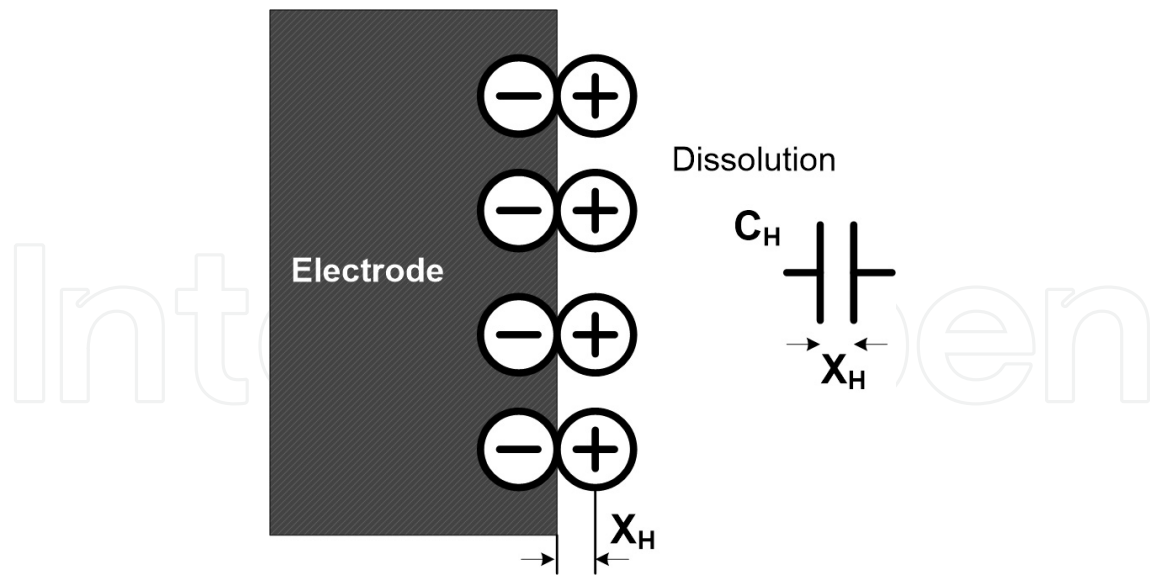
Figure 3. Classical double-layer model of a flat-parallel capacitor.

$$C_H = A \cdot \frac{\varepsilon_r \cdot \varepsilon_0}{\chi_H} \tag{1}$$

The desalination cell is built by piling several electrodes to increase the capability of water processing. In **Figure 4**, several electrodes are piled controlling the distance between them, "d," and the number of electrodes placed in series, "n."

Although there are more complex models of the ion distribution around the electrodes [10–12], the whole desalination cell can be modeled with the traditional circuit used to characterize a capacitor C. In this model two additional resistances are included, a series resistance R_S to model conduction losses, and a parallel resistance R_P that represents the self-discharge of the module.

The proposed electric model of the CDI cell (**Figure 5**) will allow the desalinization system to be simulated together with the power topology used for the energy recovery. The electrical parameters defined, R_S, R_P and C, depending on the geometrical characteristics of the CDI cell and on the salt molar concentration (M). In order to obtain their values, a current source is applied to the cell that generates a linear evolution in the voltage across the terminals.

The CDI cell is initially completely discharged. At t = 0, a constant current, I_{DC}, is applied to initiate the charging process (**Figure 6**). Therefore, since the equivalent capacitor C is initially discharged, the value of the voltage $V_C(t = 0+)$ measured will determine the value of R_S expressed in Ω.

$$R_S = \frac{\Delta V_1}{I_{DC}} \tag{2}$$

The capacitance of the CDI module, C, can be obtained from the linear charging process, during which the parallel resistance, R_P, can be neglected:
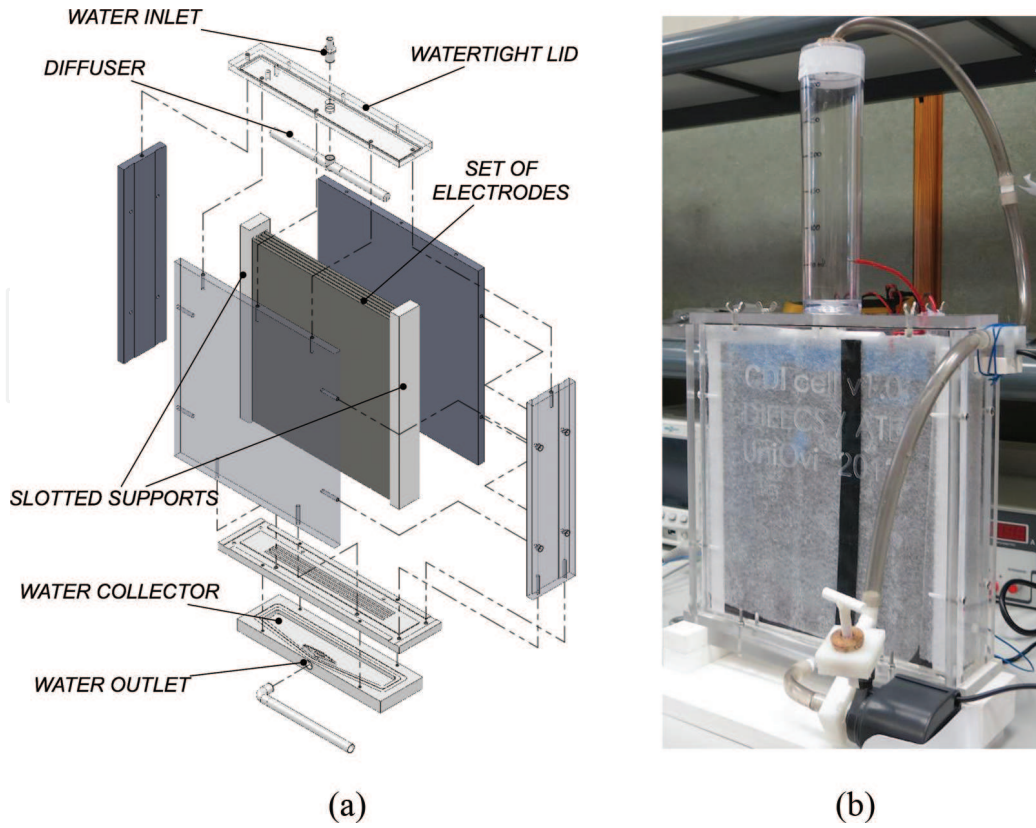
(a)   (b)

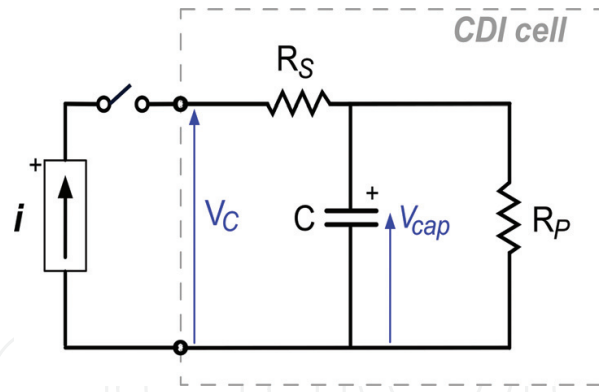**Figure 4.** (a) Schematic of a planar desalination module and (b) prototype.

Figure 5. Electric charge/discharge circuit used for the parasitic determination (R_S, R_P, C).

$$C = \frac{I_{DC}}{tg\alpha} \tag{3}$$

Finally, to determine the parallel resistance, R_P, the current source is turned off, and an exponential evolution of the voltage across the CDI cell (V_C) can be approximated by the expression:

$$V_C(t) = V_{Cmax} \cdot e^{-t/R_P \cdot C} \tag{4}$$

where V_{Cmax} is the maximum voltage across the CDI module once current I_{DC} turns to 0 A. Several tests were performed, and the absolute error obtained in the adjustment of the R_P calculation was lower than 1%.
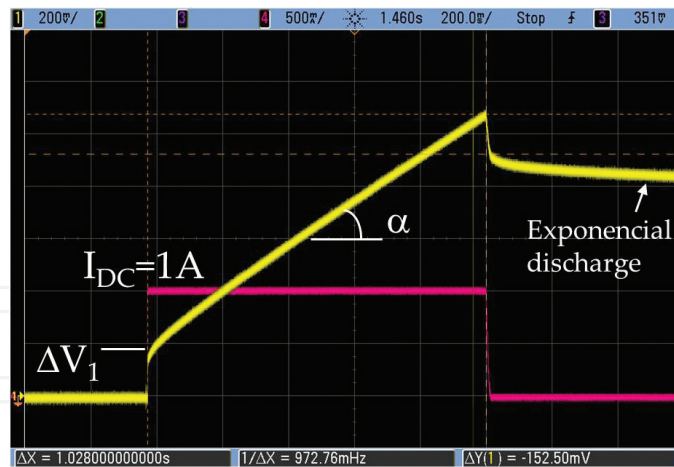
Figure 6. Electric charge/discharge test used for the parasitic determination.

With the proposed method, the values of R_S, R_P, and C can be obtained as a function of geometrical parameters: distance between electrodes "d," number of electrodes "n," the surface of electrodes "S" and NaCl molar concentration (M). To determine the tendencies of these values in an actual CDI cell, the prototype shown in **Figure 4** was built and tested.

From **Figure 7**, it can be concluded that capacity C is almost independent of the distance between electrodes.

This fact demonstrates that the capacity is mainly due to the formation of the electric double layer. The addition of several electrodes is equivalent to adding capacitors in series; therefore, the total capacity is reduced although the voltage across the cell can be increased, increasing
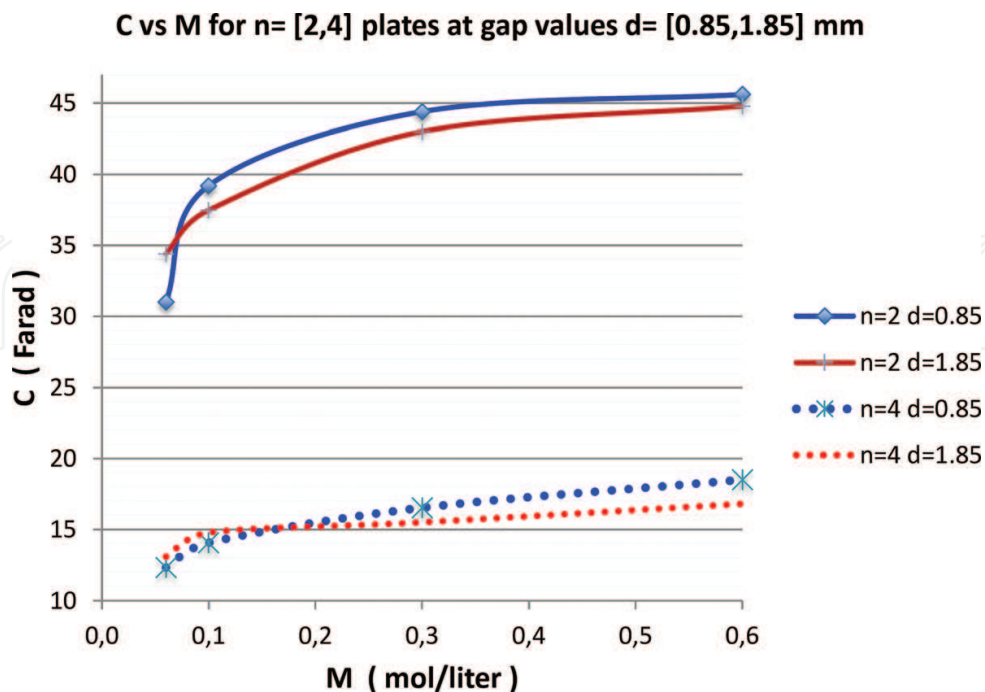

Figure 7. Capacity as a function of M (concentration of NaCl) for different configurations depending on n (number of plates-electrode) and d (distance between electrodes).
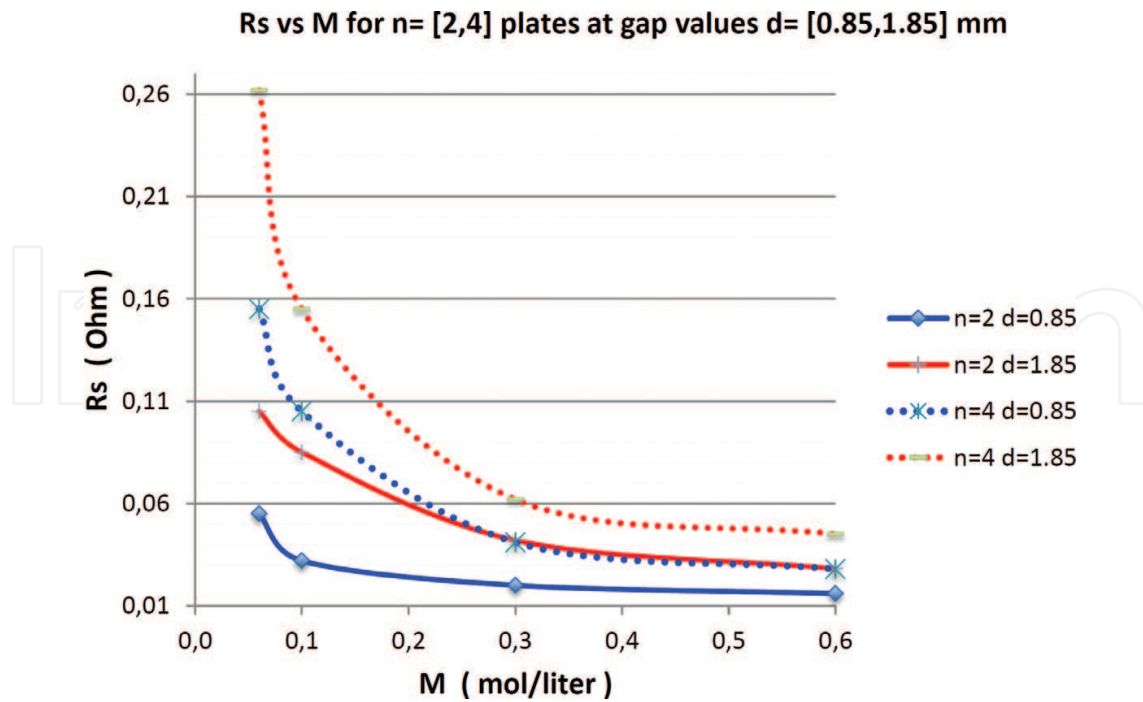
Figure 8. R_S for different configurations.

the total energy stored. For high concentrations (>0.1 to 0.6 M), the change in C is linear with a very little slope (≤1Farad per 0.1 M). This is so because the double electric layer is almost completely formed for concentrations around 0.1 M.

Regarding R_S, the series resistance (**Figure 8**), it can be seen that it increases a lot for low concentration values, M, and presents a linear trend with small or very small slope from 0.3 M on.
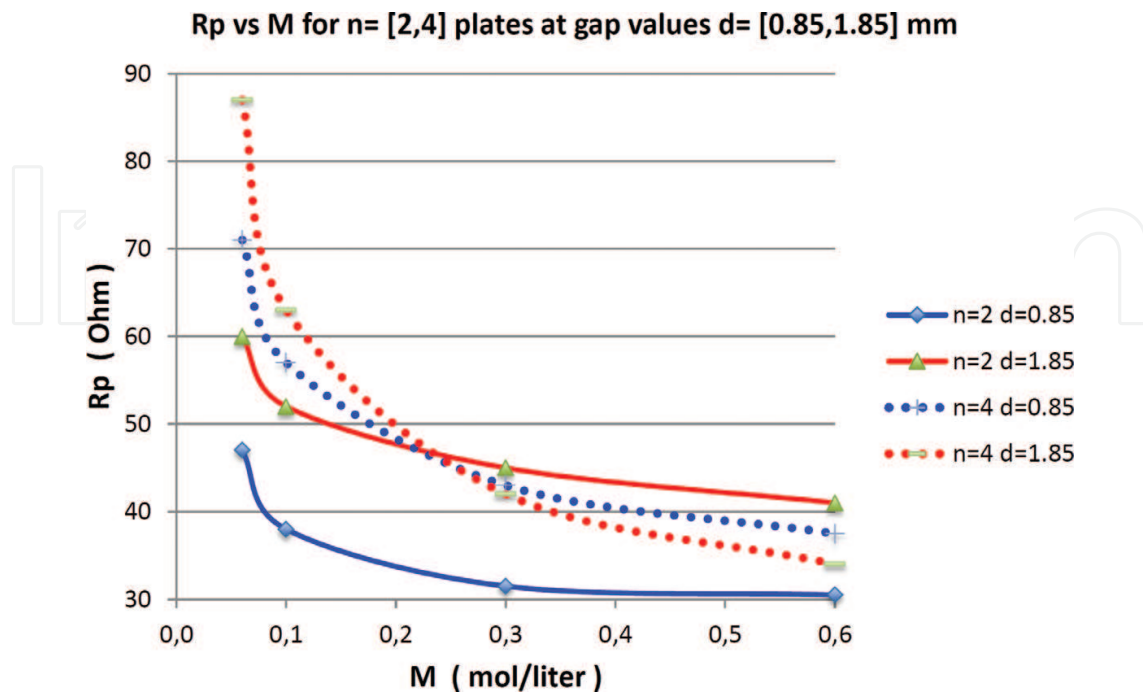

Figure 9. R_P for different configurations.

With reference to the parallel resistance, R_P, (**Figure 9**) the data measured show that it increases at low concentrations and presents a linear trend with a small or very small slope starting at 0.3 M.

4. Estimation of saline retention in electrodes

Tests have been carried out using the CDI cell shown in **Figure 4** to estimate the amount of salt that can be captured by the electrodes of this type of cells when they are completely filled with salt water. The molar salt concentration (M) is one of the parameters used to characterize the cell.

The first tests (performed at zero water flow) consist of series of charge/discharge cycles of the CDI cell using a solution with the maximum concentration considered (0.6 M).

It can be pointed out that, as shown in **Figure 10**, the electrodes present very high retention values taking into account that the initial concentration is 0.6 M. There is a variation throughout the series, tending to stabilize as the number of cycles increase.

In the second set of tests (**Figure 11**), two-electrode cells were used considering different initial concentrations, c_0, and changing the distance between electrodes (d) to identify the influence of this parameter on the salt retention. The results obtained show that salt retention increases as the distance between electrodes is reduced.

This effect can be justified if we take into account that the series resistance presented in the cell increases with the distance "d," especially at concentrations below 0.3 M, which presumably results in a decrease in the effective voltage in the electric double-layer and, as a result, a lower ionic retention.

Controlling the thickness of the nanoporous carbon layer deposited on the electrode surface, the quantity in grams of activated carbon per electrode can be determined. With the results
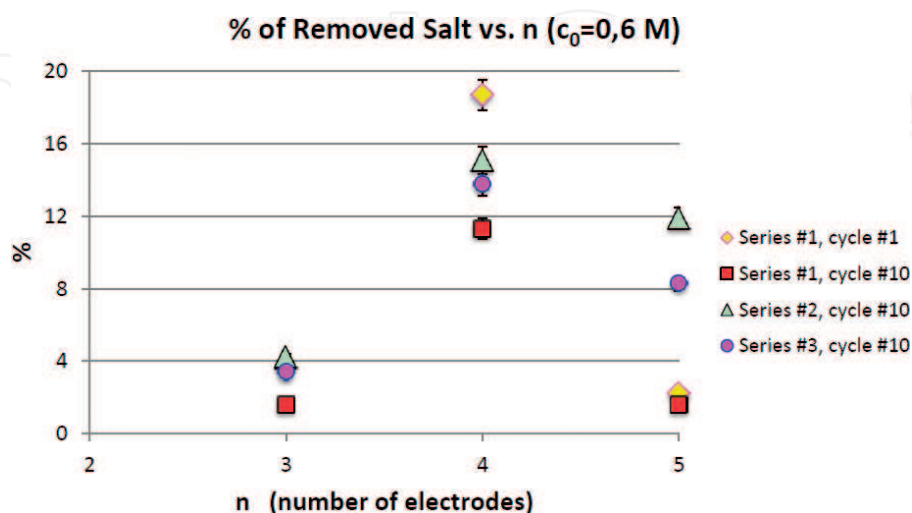

Figure 10. Results obtained by application of several charge-discharge cycles to cell configurations of more than two electrodes.
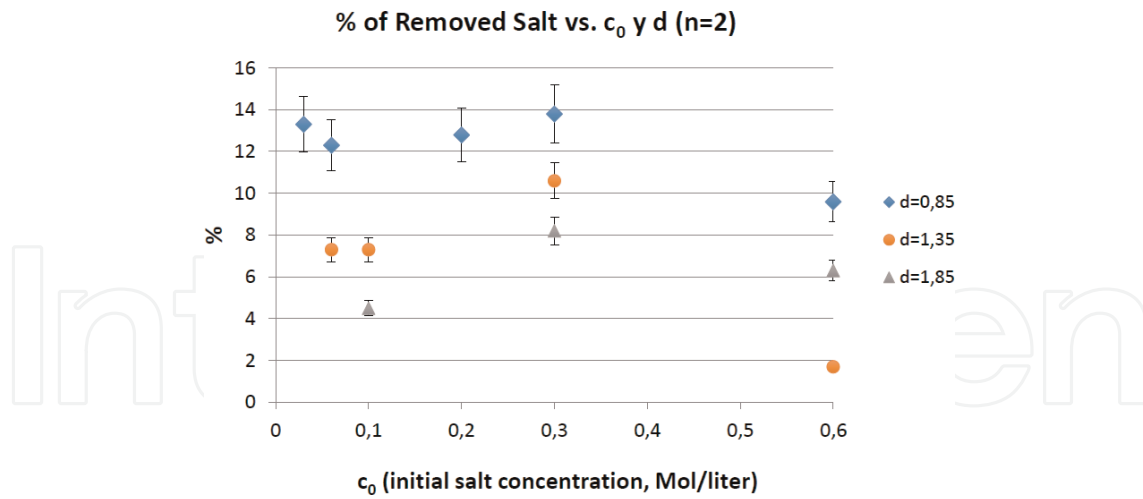
% of Removed Salt vs. c_0 y d (n=2)

Figure 11. Estimated relative retention for cell configurations of two electrodes at different separations (d) and for different initial concentrations (c_0).

obtained in the previous test, an estimation of milligrams of salt retained per gram of activated carbon was also calculated.

The data plotted in **Figure 12** are susceptible of a logarithmic adjustment in the whole range and a linear adjustment for low concentrations. Both present a good correlation ($R^2 > 0.94$).

One important parameter to be analyzed during the diffusion of ions in the charging/discharging process is the amplitude of the current used.

By reducing the amplitude of the current used during the charging process of the CDI cell, ions have a longer time to move into the carbon porosities, thus increasing the salt retention. This phenomenon seems to reach a limit at which the amount of salt retained remains the same even if the current is doubled (from $i_C = 1$ to 2 A). From this, it can be concluded that the amplitude of the charge/discharge current and the amount of salt retained are two opposed
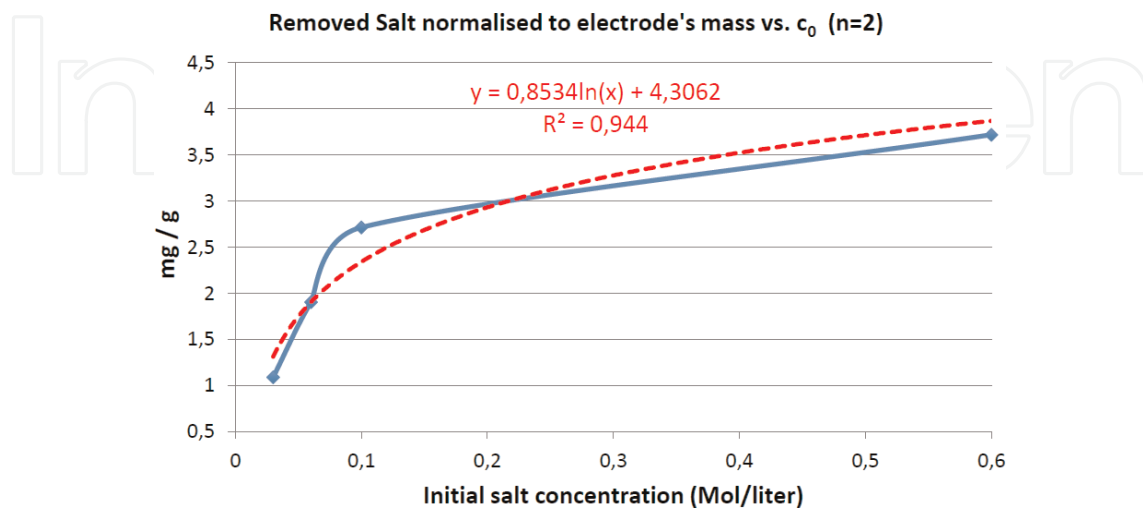
Removed Salt normalised to electrode's mass vs. c_0 (n=2)

$$y = 0{,}8534\ln(x) + 4{,}3062$$
$$R^2 = 0{,}944$$

Figure 12. Estimated relative retention for cell configurations of two electrodes and different initial concentrations (c_0).
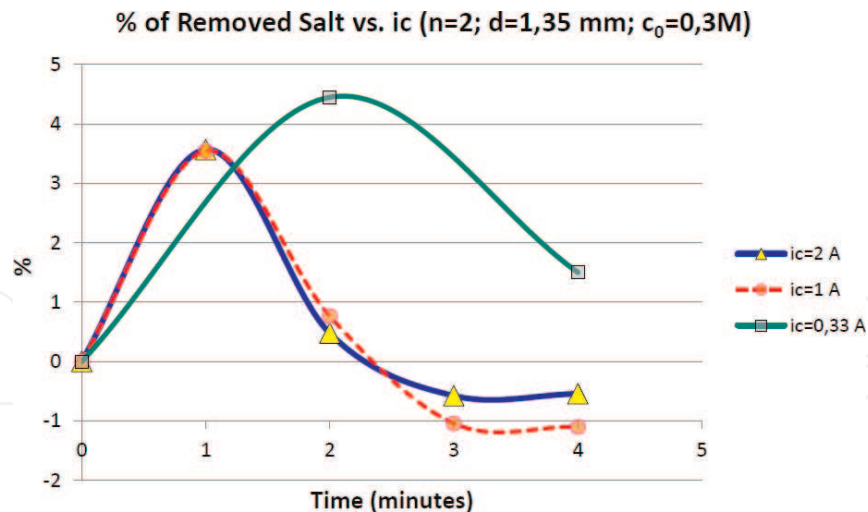
Figure 13. Estimated salt retention at different charging current (i_C).

magnitudes and a trade-off between them will be necessary. **Figure 13** also shows the time required by the electrodes to reach saturation, after which the salt retention capability drops.

5. Up/down DC/DC converter for energy recovery

As already mentioned, one of the most interesting aspects of CDI is the possibility of reusing the energy stored in capacitive cells or modules once the deionization phase has finished. The regenerative use of energy in CDI technology consists of using the energy stored in the CDI cell once it is saturated (the deionization process is finished and the cleaning process begins) and transferring it to other modules that begin their deionization phase. This strategy can be applied to several cells that exchange the energy involved in the process, thus defining a cycle to produce clean water.

In order to be able to transfer the energy stored in the CDI cell to another one, it is necessary to include a DC/DC power converter in the system (**Figure 14**).
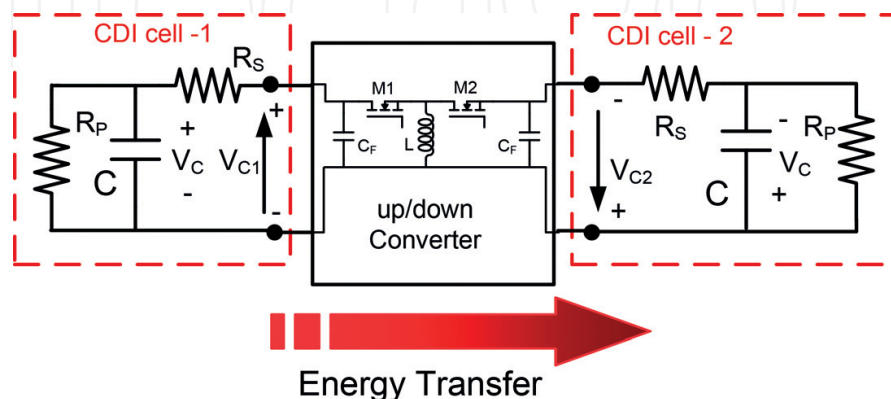

Figure 14. Desalination diagram with an up-down converter for energy transfer from CDI cell-1 to CDI cell-2.
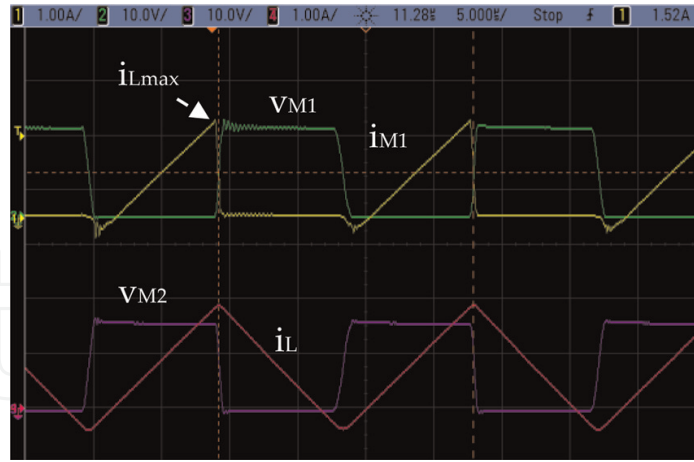
Figure 15. Voltage and current waveforms in the DC/DC converter.

One possible option for the converter topology is a buck-boost that operates at the variable frequency with hysteresis control where the maximum (i_{Lmax}) and minimum (i_{Lmin}) inductor current is fixed (**Figure 15**).

Limiting the inductor current (i_{Lmin}, i_{Lmax}) conditions the efficiency of the system, since these values are related to conduction and switching losses. The converter operation is based on transferring part of the energy stored at the input cell-1 to the inductor L during the period when transistor M1 is closed and M2 is open (t_{ON}). This period finishes when the inductor current reaches the maximum value defined by the converter control (i_{Lmax}). After this, transistor M2 is closed (M1 is opened) during time t_{OFF} and the energy stored in the inductor is discharged on the output cell-2. This stage typically finishes when the inductor current becomes equal to zero ($i_{Lmin} = 0$).

Therefore, i_{Lmax} can be used as the control parameter of the up/down converter during the energy transfer between the input CDI cell, which is completely charged, and the output CDI cell, which is initially completely discharged. By increasing the value of i_{Lmax}, the time involved in the transfer will be reduced.

To optimize the efficiency of the CDI system, it is necessary to define the value of i_{Lmax} during the energy recovery process. High values of this parameter will increase conduction losses, whereas low values of i_{Lmax} will increase the transfer time and the self-discharge through the parallel resistance R_P. On the other hand, the estimation of i_{Lmax} depends on the salt concentration (M) and the geometry of the CDI cells, which define the parameters R_P, R_S and C of the electrical model.

The DC/DC converter can be mathematically modeled assuming linear evolutions of the inductor current in each switching period (i) during the charge and discharge [13]. Therefore, when transistor M1 is conducting (M2 off), the discharge of the input cell is ideally described by:

$$uc_{1(i)} = uc_{1(i-1)} - \frac{I_{Lmax} + I_{Lmin}}{2 \cdot C} \cdot t_{on(i-1)} \tag{5}$$

Similarly, the output cell increases its voltage when M2 is on (M1 off). The equation defining such a process in each switching cycle is:

$$uc_{2(i)} = uc_{2(i-1)} + \frac{I_{Lmax} + I_{Lmin}}{2 \cdot C} \cdot t_{off(i-1)} \tag{6}$$

The RMS currents through the cells in each switching period can also be determined by:

$$i_{RMSC1_i} = \sqrt{\frac{1}{ton_i + toff_i} \cdot \int_0^{ton_i} \left(\frac{I_{max} - I_{min}}{ton_i} \cdot t + I_{min} \right)^2 \cdot dt} \tag{7}$$

$$i_{RMSC2_i} = \sqrt{\frac{1}{ton_i + toff_i} \cdot \int_{ton_i}^{ton_i + toff_i} \left(\frac{I_{min} - I_{max}}{toff_i} \cdot (t - ton_i) + I_{max} \right)^2 \cdot dt} \tag{8}$$

Based on the RMS current values calculated with the equations above, conduction and switching losses can be estimated:

$$P_{cond} = \frac{\sum_i \left(i_{RMSC1i}^2 + i_{RMSC2i}^2 \right) \cdot (ton_i + toff_i) \cdot R}{T_{total}} \tag{9}$$

$$P_{switch} = \frac{\frac{1}{2} \cdot (tr + tf) \sum_i \begin{pmatrix} I_{min} \cdot \left(uc_{1i} + uc_{2(i+1)} \right) + \\ I_{max} \cdot \left(uc_{1(i+1)} + uc_{2i} \right) \end{pmatrix}}{T_{total}} \tag{10}$$

The parameter R represents the total series resistance along the conduction path.

Voltage losses due to cell self-discharge are also taken into account in the model by incorporating the following expression that represents the energy lost in a cell during the switching period "i" due to self-discharge:

$$E_{C_{Rp}i} = \frac{1}{R_P} \cdot uc_i^2 \left(t_{ON_i} + t_{OFF_i} \right) \tag{11}$$

Once the energy dissipated in each cycle (E_{Ccond}: energy loosed during conduction stage, $E_{Cswitch}$: energy loosed during switching stage, E_{Cp}: energy loosed in R_P) is known, the real voltages of capacitors C1 and C2 can be recalculated as follows:

$$\Delta E_{C1i} = \frac{1}{2} \cdot C1 \cdot uc_{1(i+1)}^2 - \frac{1}{2} \cdot C1 \cdot uc_{1i}^2 \tag{12}$$

$$\Delta E_{C2i} = \frac{1}{2} \cdot C2 \cdot uc_{2(i+1)}^2 - \frac{1}{2} \cdot C2 \cdot uc_{2i}^2 \tag{13}$$

$$\Delta Ereal_{C1i} = \Delta E_{C1i} - E_{C1cond_i} - E_{C1switch_i} - E_{C_{Rp_i}} \tag{14}$$

$$\Delta Ereal_{C2i} = \Delta E_{C2i} - E_{C2cond_i} - E_{C2switch_i} - E_{C_{Rp_i}} \tag{15}$$

From the previous expressions, the real voltage across each capacitor can be derived:

$$uc_{1(i+1)_{real}} = \sqrt{\frac{2 \cdot \left(\Delta Ereal_{C1i} + \frac{1}{2} \cdot C1 \cdot uc_{1i_{real}}^2\right)}{C1}} \tag{16}$$

$$uc_{2(i+1)_{real}} = \sqrt{\frac{2 \cdot \left(\Delta Ereal_{C2i} + \frac{1}{2} \cdot C2 \cdot uc_{2i_{real}}^2\right)}{C2}} \tag{17}$$

The model described allows users to obtain a large amount of information related to the behavior of the converter: currents, voltages, transfer times, performance. But it can also provide insight into the influence that the desalination cells will have on these parameters. In order for this to be possible, the previous expressions must include the influence of the distance between electrodes "d," the number of electrodes "n," the molarity "M," and the S surface.

$$E_{Rson(i)}(d, n, M, S) = R_S(d, n, M, S) \cdot \left(i_{RMSC1_{(i)}}\right)^2 \cdot t_{on} \tag{18}$$

$$E_{Rsoff(i)}(d, n, M, S) = R_S(d, n, M, S) \cdot \left(i_{RMSC2_{(i)}}\right)^2 \cdot t_{off} \tag{19}$$

$$E_{R_S(i)}(d, n, M, S) = E_{Rson(i)}(d, n, M, S) + E_{Rsoff(i)}(d, n, M, S) \tag{20}$$

$$E_{R_{P(i)}}(d, n, M) = \int_0^{T_{(i)}} \frac{\left[u_{C(i)}(t)\right]^2}{R_P(d, n, M)} \cdot dt \tag{21}$$

$$E_{T(i)}(d, n, M, S) = E_{R_{S(i)}}(d, n, M, S) + E_{R_{P(i)}}(d, n, M, S) + P_{cond(i)}(d, n, M, S) \cdot T + P_{switch(i)}(d, n, M, S) \cdot T \tag{22}$$

From the equation system described above, it is possible to determine the overall efficiency of the DC/DC converter together with the desalination cells [14].

Once the equations to calculate losses have been established, it is possible to determine the optimum i_{Lmax} current in each switching period by implementing an iterative process according to the flow chart of **Figure 16**. The procedure consists in increasing the value of i_{Lmax} in each switching period until the maximum efficiency is obtained for that switching period. After that, a new switching period is considered and a new iteration with i_{Lmax} is carried out in order to derive the optimum i_{Lmax} value for the new switching period. The process is repeated until the input CDI cell is completely discharged.

The process mentioned was applied to several cell configurations consisting of four electrodes of 250×250×5mm placed at different distances from one another, in which the salt concentration was also a parameter under control [14]. As an example, **Figure 17** shows the optimal current when the cell parameters associated with this configuration are: C = 0.1F, Rs = 25mΩ, and Rp = 40 Ω. Taking these parameters into account, the calculation of the optimum current as indicated above gives rise to the evolution shown in **Figure 17**.
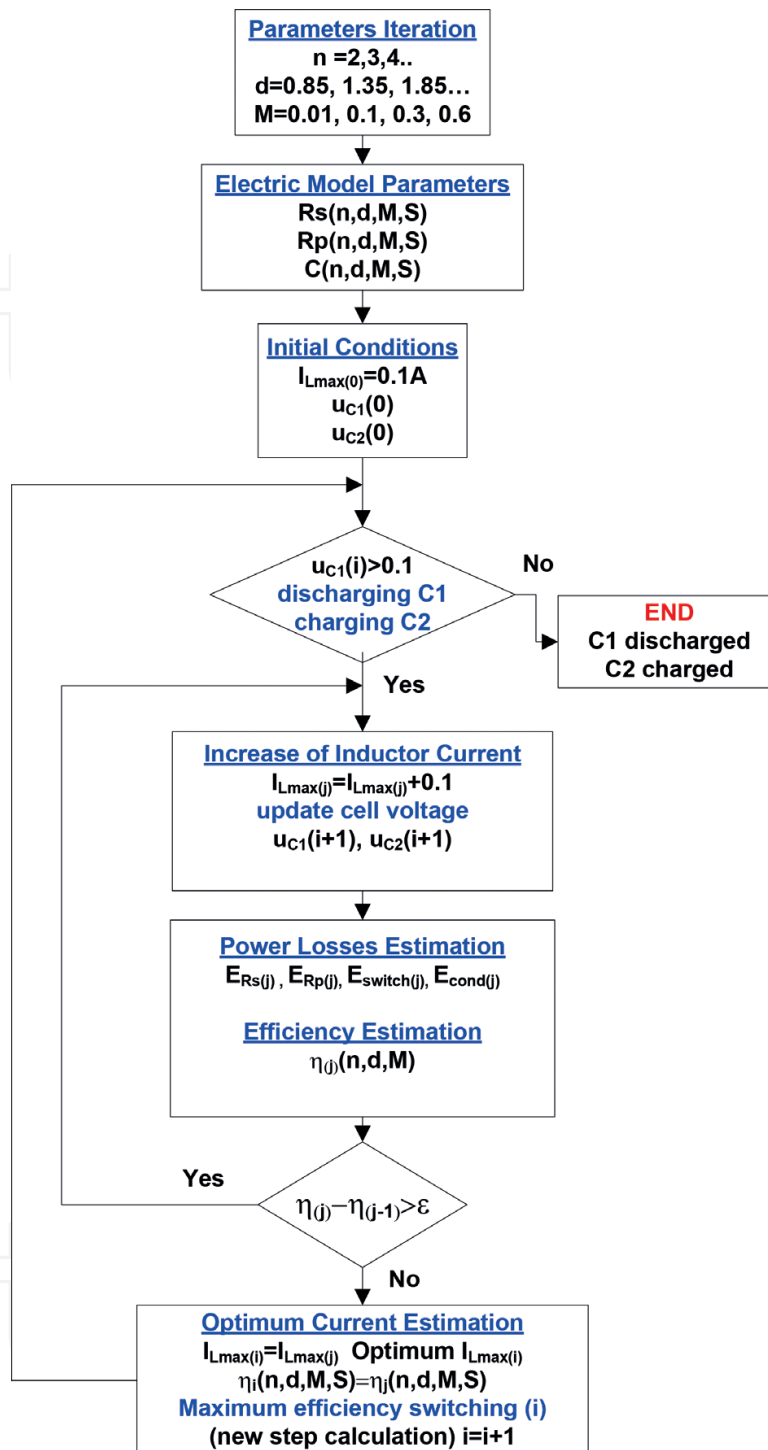
Figure 16. Optimum current i_{Lmax} estimation flow chart per switching period.

By controlling the switching times of the semiconductors it is possible to control that the maximum current through the inductor follows the profile defined by the optimum current for each specific cell. **Figure 18** shows the efficiency obtained in several cases when the optimal current is used and the maximum voltage is 1.5 V. It is important to point out the necessity of reducing the series resistance because it limits the maximum efficiency that can be obtained.
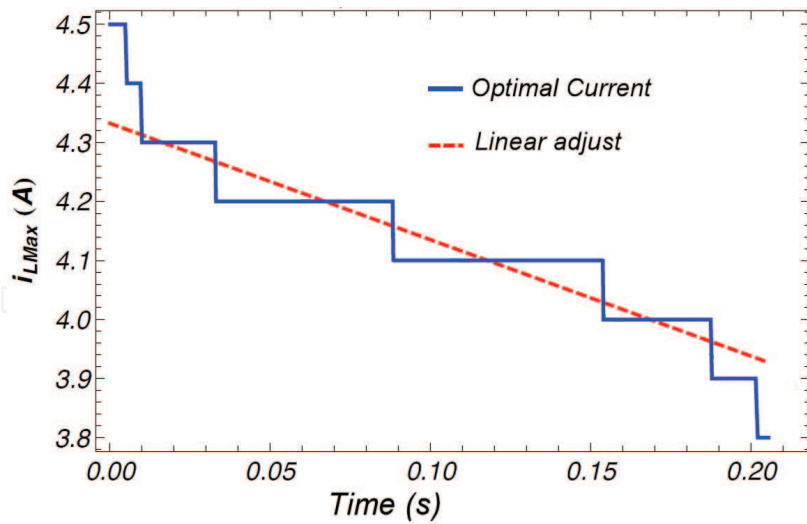
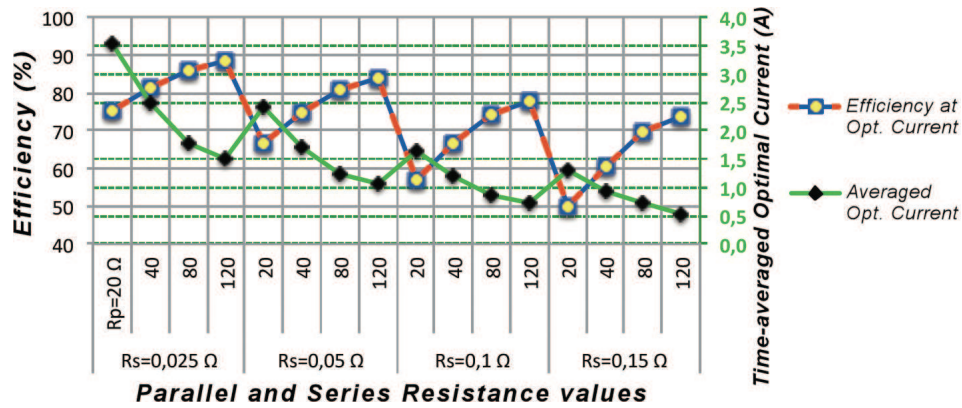**Figure 17.** Optimum current i_{Lmax} estimated.

Figure 18. System efficiency operating at optimum current (red) and average optimum current during the energy transference (green).

The green plot determines the average of the optimal current during the whole energy transference process (right-hand scale).

The efficiency improvement depends on the CDI cell geometry and the salt concentration (M) because these magnitudes condition the values of the parameters that define the electrical model of the cell. Actual measurements confirmed that, by applying this control strategy, the efficiency was improved by 10% in most of the cases as compared to that obtained when using a constant current value during the charge/discharge process.

6. Conclusions

The method presented allows the electrical characterization of the CDI cell in terms of salt concentration in the water and cell geometry. A model proposed is based only on three parameters R_P, R_S, C, which simplifies mathematical calculations. Using this electrical model

and the mathematical characterization of the DC/DC converter, it is possible to identify energy losses in the cell either by self-discharge or due to the current handled during the energy recovery processes, together with the power losses in the converter.

As a result, a clear identification of the power losses in all the system components is obtained. This makes it possible to identify the optimum current to minimize losses and optimize process efficiency for any salt concentration once the cell geometry is defined.

The feedback parameter used by the converter control strategy described is the maximum current through the inductor, i_{Lmax}. This parameter is calculated at each switching period so as to obtain the optimum value that maximizes the efficiency of the energy transfer between CDI cells.

Author details

Alberto M. Pernía*, Miguel J. Prieto, Juan A. Martín-Ramos, Pedro J. Villegas and Francisco J. Álvarez-González

*Address all correspondence to: amartinp@uniovi.es

University of Oviedo, Gijón, Spain

References

[1] UN-Water. Water in a Changing World. The United Nations World Water Development Report 3. UNESCO Publishing; Mar 2009. http://publishing.unesco.org/

[2] Younos T, Tulou KE. Overview of desalination techniques. Journal of Contemporary Water Research and Education. 2009;**132**:3-10

[3] Fraidenraich N, Vilela OC, Lima GA, Gordon JM. Reverse osmosis desalination: Modeling and experiment. Applied Physics Letters. 2009;**94**:124102-124103

[4] Oren Y. Capacitive deionization (CDI) for desalination and water treatment-past, present and future (a review). Desalination. 2008;**228**:10-29

[5] Gao Y, Li HB, Cheng ZJ, Zhang MC, Zhang YP, Zhang ZJ, Cheng YW, Pan LK, Sun Z. Electrosorption of cupric ions from solutions by carbon nanotubes and nanofibres film electrodes grown on graphite substrates. In: Proceedings of the IEEE Nanoelectronics Conference INEC 2008; Shanghai, China; 24–27 March 2008. pp. 242-247

[6] Hwang S, Hyun S. Capacitance control of carbon aerogel electrodes. Journal of Non-Crystalline Solids. 2004;**347**:238-245

[7] Xu P, Drewes JE, Heil D, Wang G. Treatment of brackish produced water using carbon aerogel-based capacitive deionization technology. Water Research. 2008;**42**:2605-2617

[8]   Li H, Zou L. Ion-exchange membrane capacitive deionization: A new strategy for brackish water desalination. Desalination. 2011;**275**(1-3):62-66

[9]   Hassanvanda A, Chenb GQ, Webleya PA, Sandra E. Kentish improvement of MCDI operation and design through experiment and modelling: Regeneration with brine and optimum residence time. Desalination. September 2017;**417**(1):36-51

[10] Niu R, Yang H. Modeling and identification of electric double-layer supercapacitors. ICRA Communications. Feb. 2011:1-4

[11] Spyker RL, Nelms RM. Classical equivalent circuit parameters for a double-layer capacitor. IEEE Transactions on Aerospace and Electronic Systems. Jul. 2000;**36**(3):829-836

[12] Hemmatifar A, Stadermann M, Santiago JG. Two-dimensional porous electrode model for capacitive deionization. The Journal of Physical Chemistry C. 2015;**119**(44):24681-24694

[13] Pernia AM, Norniella JG, Martin-Ramos JA, Diaz J, Martinez JA. Up-down converter for energy recovery in a CDI desalination system. IEEE Transactions on Power Electronics. July 2012;**27**(7):3257-3265

[14] Álvarez-González FJ, Martín-Ramos JA, Díaz J, Martínez JA, Pernía AM. Energy-recovery optimization of an experimental CDI desalination system. IEEE Transactions on Industrial Electronics. March 2016;**63**(3):1586-1597